Observations of Sweep–Ejection Dynamics for Heat and Momentum Fluxes during Wildland Fires in Forested and Grassland Environments

WARREN E. HEILMAN,[a] TIRTHA BANERJEE,[b] CRAIG B. CLEMENTS,[c] KENNETH L. CLARK,[d] SHIYUAN ZHONG,[e] AND XINDI BIAN[a]

[a] *USDA Forest Service Northern Research Station, Lansing, Michigan*
[b] *Department of Civil and Environmental Engineering, University of California, Irvine, Irvine, California*
[c] *Department of Meteorology and Climate Science, San José State University, San Jose, California*
[d] *USDA Forest Service Northern Research Station, New Lisbon, New Jersey*
[e] *Department of Geography, Environment, and Spatial Sciences, Michigan State University, East Lansing, Michigan*

(Manuscript received 3 April 2020, in final form 1 September 2020)

ABSTRACT: The vertical turbulent transfer of heat and momentum in the lower atmospheric boundary layer is accomplished through intermittent sweep, ejection, outward interaction, and inward interaction events associated with turbulent updrafts and downdrafts. These events, collectively referred to as sweep–ejection dynamics, have been studied extensively in forested and nonforested environments and reported in the literature. However, little is known about the sweep–ejection dynamics that occur in response to turbulence regimes induced by wildland fires in forested and nonforested environments. This study attempts to fill some of that knowledge gap through analyses of turbulence data previously collected during three wildland (prescribed) fires that occurred in grassland and forested environments in Texas and New Jersey. Tower-based high-frequency (10 or 20 Hz) three-dimensional wind-velocity and temperature measurements are used to examine frequencies of occurrence of sweep, ejection, outward interaction, and inward interaction events and their actual contributions to the mean vertical turbulent fluxes of heat and momentum before, during, and after the passage of fire fronts. The observational results suggest that wildland fires in these environments can substantially change the sweep–ejection dynamics for turbulent heat and momentum fluxes that typically occur when no fires are present, especially the relative contributions of sweeps versus ejections in determining overall heat and momentum fluxes.

KEYWORDS: Forest canopy; Eddies; Fluxes; Turbulence; Field experiments; Forest fires; Vegetation–atmosphere interactions

1. Introduction

The turbulent transfer of heat and momentum in the lower atmospheric boundary layer (ABL) is known to be a highly intermittent process (Shaw et al. 1983) and is associated with coherent turbulent structures or eddy motions characterized primarily by updrafts and downdrafts, also known as ejections and sweeps, respectively (Katul et al. 1997). These turbulent updrafts and downdrafts redistribute scalars such as heat and momentum in the atmospheric surface layer. Numerous observational and modeling studies of the atmospheric sweep–ejection dynamics that occur within and above surface vegetation layers have been conducted over the last four decades, often drawing upon previous analysis techniques developed for examining the sweep–ejection dynamics in pipe and channel flow. Wallace (2016) provided an historical summary and listing of many of these pipe flow, streamflow, and atmospheric boundary layer studies.

Some of the key results from previous sweep–ejection studies that focused on daytime turbulent momentum fluxes in the lower ABL suggest that 1) ejections (i.e., the upward flux of low horizontal momentum air) dominate or are as significant as sweeps (i.e., the downward flux of high horizontal momentum air) within sparse canopy layers, in areas well above canopy layers, and above relatively smooth or bare terrain (e.g., Raupach 1981; Poggi et al. 2004; Katul et al. 2006; Poggi and Katul 2007; Thomas and Foken 2007); 2) sweeps are the dominant vertical turbulent momentum-flux process within dense canopy layers (e.g., Shaw et al. 1983; Baldocchi and Meyers 1988; Katul and Albertson 1998; Su et al. 1998; Finnigan 2000; Katul et al. 2006; Banerjee et al. 2017); and 3) extreme but relatively infrequent sweep, ejection, outward interaction (i.e., the upward flux of high horizontal momentum air), and inward interaction (i.e., the downward flux of low momentum air) events contribute a disproportionate amount to the total vertical turbulent momentum-flux fields within canopy layers (e.g., Finnigan 1979; Shaw et al. 1983; Baldocchi and Hutchison 1987; Baldocchi and Meyers 1988; Bergström and Högström 1989).

Studies of sweep–ejection dynamics addressing daytime vertical turbulent heat fluxes in the lower ABL have also been reported in the literature, but the studies yielded results that are somewhat inconsistent as noted by Katul et al. (1997). For example, Bergström and Högström (1989) found that ejections (i.e., the upward turbulent flux of warm air) tended to be the largest contributor to the total vertical turbulent heat-flux fields within and immediately above a pine forest canopy. On the other hand, Maitani and Shaw (1990) found that the contribution of sweeps (i.e., the downward turbulent flux of cool air) was much larger than the contribution from ejections within a deciduous forest canopy, but at heights roughly 2 times the height of treetops, low-frequency (large eddy) ejection

Corresponding author: Warren E. Heilman, warren.heilman@usda.gov

DOI: 10.1175/JAMC-D-20-0086.1

events were dominant. The studies of Chen (1990) and Maitani and Ohtaki (1987) suggested that vertical turbulent heat fluxes over rough surfaces like shrub-covered land and fluxes over bare soil and paddy fields in unstable surface layers tended to be dominated by ejections instead of sweeps. Similar to vertical turbulent momentum fluxes in the lower ABL, Bergström and Högström (1989) found extreme and relatively infrequent ejection, sweep, outward interaction, and inward interaction events typically contribute a disproportionate amount to the total vertical turbulent heat-flux fields within forest vegetation layers.

Although studies of sweep–ejection dynamics in the lower ABL have been numerous over the last four decades, little is known about the sweep–ejection dynamics that occur in the highly perturbed environment surrounding wildland fires. Beer (1991) and Pimont et al. (2009) noted that coherent turbulent structures leading to turbulent heat- and momentum-flux sweep and ejection events within forest vegetation layers have the potential for affecting the spread of wildland fires through surface fuel beds and overstory vegetation. Mueller et al. (2014) also stressed the importance of sweep–ejection dynamics for momentum fluxes within forest vegetation layers when modeling canopy flow for predictions of wildland fire spread via systems like the Wildland-Urban Interface Fire Dynamics Simulator (WFDS) (Mell et al. 2007, 2009). Many of the recent observational studies of atmospheric turbulence regimes in wildland fire environments (e.g., Clements et al. 2007; Seto et al. 2013; Heilman et al. 2015, 2017, 2019) suggest that the typical ambient sweep–ejection dynamics that govern turbulent transfer of heat and momentum in atmospheric surface layers over areas of flat and complex terrain and over vegetated and nonvegetated surfaces are likely to be significantly modified when wildland fires are present.

In this study, we investigate the sweep–ejection dynamics that occurred during three wildland (prescribed) fire experiments, two of them in forested environments in the state of New Jersey and one in a grassland environment in the state of Texas. This study represents an extension of the Clements et al. (2007, 2008) and Heilman et al. (2015, 2017, 2019) studies, which focused on other properties of the local turbulence regimes that developed during the fire experiments. The sections below provide a short overview of the prescribed fire events, a description of the method used for examining sweep–ejection dynamics during the fire events, a presentation of the observational results, and a discussion of the relevance of the results for wildland fire behavior and smoke dispersion in forested and grassland environments.

2. Methods

a. Overview of prescribed fire experiments

On 23 February 2006, the well-known FireFlux I grassland prescribed fire experiment was conducted at the Houston Coastal Center (HCC) near La Marque, Texas, as part of the HCC's fuel management strategies (Clements et al. 2007). For this experiment, a 40-ha native grassland plot [average grass height (h_g): 1.5 m; average fuel loading: 1.08 kg m^{-2}] containing big bluestem (*Andropogon gerardi*), little bluestem (*Schizachyrium scoparium*) and longspike tridens (*Tridens strictus*) was instrumented with sonic anemometers and other monitoring equipment mounted at multiple levels on a 43-m tower and a 10-m tower set up in the interior of the plot (see Fig. 1 in Clements et al. 2007). This instrumentation provided high-frequency (20 Hz) measurements of zonal U, meridional V, and vertical W velocity components and temperatures T at heights AGL (z) of 2.1 m ($z/h_g = 1.4$), 10 m ($z/h_g = 6.7$), 28.5 m ($z/h_g = 19$), and 43 m ($z/h_g = 28.7$) on the 43-m tower and at 2.3 m ($z/h_g = 1.5$) and 10 m ($z/h_g = 6.7$) on the 10-m tower during the experiment.

At 1243 LT on 23 February 2006, a line fire was ignited along the northern boundary of the burn block under ambient near-surface northeasterly winds at approximately 3 m s^{-1}, leading to a head fire with flame lengths of 5.1 m that spread through the block and instrumented towers from north to south at an average rate of 40.8 m min^{-1} and intensity of 3200 kW m^{-1} (Clements 2007). Consumption of the grass fuel was not measured, but it was estimated at 90% of the initial fuel loading based on postburn visual observations. The horizontal and vertical velocity components and temperature measurements obtained from the sonic anemometers mounted on the 43-m tower were used for the sweep–ejection analyses conducted in this study. Note that the 2.1-m AGL monitoring level was less than the 5.1-m flame lengths of the line fire. However, the grass surrounding the 43-m tower was mowed out to a distance of 5 m from the base of the tower to minimize potential instrument damage and the occurrence of flames impinging on the low-level instrumentation. For a complete description of the FireFlux I experiment, see Clements et al. (2007).

Two prescribed fire experiments with similar monitoring strategies to that of the FireFlux I experiment in Texas were conducted in 2011 and 2012 in New Jersey. On 20 March 2011 and 6 March 2012, prescribed burns were carried out in the New Jersey Pinelands National Reserve by the New Jersey Forest Fire Service as part of their overall strategy to manage surface fuels in the New Jersey Pine Barrens (https://www.state.nj.us/dep/parksandforests/fire/whm-burning.htm). The burn block areas for the 2011 and 2012 experiments were 107 and 97 ha, respectively. Forest overstory vegetation in both burn blocks was composed of pitch pine (*Pinus rigida* Mill.), shortleaf pine (*P. echinata* Mill.), and mixed oak (*Quercus* spp.); the understory vegetation (2011 average fuel loading: 1.485 kg m^{-2}; 2012 average fuel loading: 1.104 kg m^{-2}) was composed of blueberry (*Vaccinium* spp.), huckleberry (*Gaylussacia* spp.), and scrub oak. Overstory vegetation heights h_o ranged from 15 to 23 m (20-m average height) in both blocks, while understory vegetation heights h_u ranged from 0.5 to 1.5 m (1.0-m average height) and from 0.3 to 1.0 m (0.7-m average height) for the 2011 and 2012 blocks, respectively. Deciduous vegetation in the plots had not leafed out yet. The block-averaged plant-area-density profiles of the forest overstory vegetation in the 2011 and 2012 burn blocks, derived from canopy density measurements using lidar remote sensing techniques (Skowronski et al. 2011) and reported in Charney et al. (2019), exhibited maximum values of 0.06 and 0.05 m^2 m^{-3}, respectively, at about 10 m AGL (see Fig. 1 in Charney et al. 2019).

Both burn blocks were instrumented with sonic anemometers, thermocouples, and a variety of other instruments mounted on

TABLE 1. Summary features of the 2006 Texas prescribed grass-fire experiment (TX2006) and the 2011 and 2012 New Jersey prescribed understory-fire experiments (NJ2011; NJ2012).

Feature	TX2006	NJ2011	NJ2012
Date	23 Feb 2006	20 Mar 2011	6 Mar 2012
Plot size	40 ha	107 ha	97 ha
Overstory vegetation	—	Pitch/shortleaf pine; mixed oak	Pitch/shortleaf pine; mixed oak
Overstory vegetation height (h_o)	—	15–23 m	15–23 m
Understory/grass vegetation	Big bluestem grass, little bluestem grass, and longspike tridens	Blueberry, huckleberry, and scrub oak	Blueberry, huckleberry, and scrub oak
Understory/grass vegetation height (h_u or h_g)	1.5 m	1.0 m	0.7 m
Surface fuel loading	1.080 kg m^{-2}	1.485 kg m^{-2}	1.104 kg m^{-2}
Ambient wind speed	3 m s^{-1} (2.1 m AGL)	3 m s^{-1} (3 m AGL)	3 m s^{-1} (3 m AGL)
Ambient wind direction	Northeast (45°)	Northeast–southeast (45°–135°)	Southwest–northwest (225°–315°)
Burn type	Heading	Backing	Backing
Fire intensity	3200 kW m^{-1}	325 kW m^{-1}	52 kW m^{-1}
Spread rate	40.80 m min^{-1}	1.50 m min^{-1}	0.33 m min^{-1}
Flame length	5.1 m	1.0 m	0.5 m
Fuel consumption	—	696 g m^{-2}	507 g m^{-2}

10-, 20-, and 30-m towers set up in their interiors (Heilman et al. 2013, 2015). This instrumentation provided atmospheric measurements required for a broader U.S. Joint Fire Science Program study focused on fire-fuel-atmosphere interactions and smoke dispersion during the fire events. The sonic anemometers yielded high-frequency (10 Hz) measurements of the zonal, meridional, and vertical velocity components and temperatures at multiple vertical levels AGL [3 m: $z/h_u = 3$ (2011), $z/h_u = 4.3$ (2012), and $z/h_o = 0.15$; 10 m: $z/h_u = 10$ (2011), $z/h_u = 14.3$ (2012), and $z/h_o = 0.5$; 20 m: $z/h_u = 20$ (2011), $z/h_u = 28.6$ (2012), and $z/h_o = 1$; and 30 m: $z/h_u = 30$ (2011), $z/h_u = 42.9$ (2012), and $z/h_o = 1.5$] during the prescribed fire events. Although the 10-Hz sampling frequency was less than the preferred 20-Hz sampling frequency adopted for the FireFlux I experiment, only 10-Hz data were available from the New Jersey fire experiments. For consistency with the previous turbulence regime analyses carried out for the two New Jersey fire experiments as outlined in Heilman et al. (2015, 2017, 2019), measurements from the 20-m tower sonic anemometers (3, 10, and 20 m AGL) served as the basis for the turbulent heat- and momentum-flux sweep–ejection analyses performed for this study.

The New Jersey Forest Fire Service initiated a backing line fire along the western boundary of the 2011 burn block (initial ignition at 0955 LT; northeasterly to southeasterly ambient near-surface winds at approximately 3 m s^{-1}) and multiple backing line fires along the eastern boundary and along north–south-oriented plow lines of the 2012 burn block (initial ignition at 0930 LT; northwesterly to southwesterly ambient near-surface winds at approximately 3 m s^{-1}). The line fires were allowed to spread against the ambient winds and through the instrumented towers set up in the interior of the burn blocks. Fire-spread rates and intensities were much lower than for the FireFlux I grass-fire experiment. Average line-fire-spread rates (intensities) were 1.5 m min^{-1} (325 kW m^{-1}) and 0.33 m min^{-1} (52 kW m^{-1}) for the 2011 and 2012 fire events, respectively, with 1–2 m average line-fire widths for both events. Only understory fuels were consumed [average understory consumption: (2011) 696 g m^{-2}; (2012) 507 g m^{-2}]; no overstory vegetation burning took place. Estimated flame lengths for the 2011 and 2012 experiments were 1.0 and 0.5 m, respectively. Comprehensive descriptions of both prescribed fire events, including maps of the burn blocks and monitoring networks, can be found in Heilman et al. (2013, 2015) and are not repeated here.

A summary of the key features of the 2006 Texas and the 2011 and 2012 New Jersey prescribed fire experiments is provided in Table 1. Hereinafter, the 2006 Texas grass-fire experiment is referred to as TX2006, and the 2011 and 2012 New Jersey understory-fire experiments are referred to as NJ2011 and NJ2012, respectively.

b. *Data processing*

The high-frequency velocity component and temperature raw data obtained from the sonic anemometers on the 43-m tower for the TX2006 experiment and the 20-m towers for the NJ2011/NJ2012 experiments underwent quality-assurance/quality-control (QA/QC) processing to remove spurious values as well as tilt-correction processing (Wilczak et al. 2001) to minimize potential vertical velocity measurement errors associated with sonic anemometers not mounted exactly level on the towers. Because of the very high intensity of the TX2006 grass fire (3200 kW m^{-1}), sonic anemometer measurements of wind velocities and temperatures on the 43-m tower when the line fire was near the tower were limited due to instrument errors associated with their operation in the harsh environment; only measurements when temperatures were below 50°C were found to be viable. Although this limited the amount of data available for assessing the sweep–ejection dynamics in the near vicinity of the grass fire, overall characteristics of behavior of the sweep–ejection dynamics and comparisons of those dynamics between grass-fire and understory-fire

environments were still possible, as described in the Results and Discussion section below. For reference, thorough descriptions of the data processing steps for the TX2006, NJ2011 and NJ2012 experiments are reported in Clements et al. (2008) and Heilman et al. (2015).

Following the QA/QC and tilt correction procedures, instantaneous (10 or 20 Hz) horizontal streamwise velocity magnitudes (S) were computed from the instantaneous U and V velocity components:

$$S = (U^2 + V^2)^{0.5}. \tag{1}$$

Then, perturbation horizontal streamwise velocities s', perturbation vertical velocities w', and perturbation temperatures t' for each experiment were computed by subtracting time-period-specific mean horizontal streamwise velocity magnitudes $\overline{S}$, mean vertical velocities $\overline{W}$, and mean temperatures $\overline{T}$ from the raw 20-Hz (TX2006) or 10-Hz (NJ2011/NJ2012) velocity and temperature values (S, W, and T), respectively. Mean (block average) velocities and temperatures were calculated over defined periods before and after defined fire-front-passage (FFP) periods at the tower sites. For TX2006, the pre-FFP, FFP, and post-FFP time periods were set at 1200–1243 LT (43.5 min), 1243–1249 LT (6 min), and 1249–1306 LT (16.5 min), respectively. For NJ2011, the pre-FFP, FFP, and post-FFP periods were set at 1435–1505 LT (30 min), 1505–1535 LT (30 min), and 1535–1605 LT (30 min), respectively, and the corresponding NJ2012 periods were set at 1452–1522 LT (30 min), 1522–1552 LT (30 min), and 1552–1622 LT (30 min). Note that the period intervals were set on the basis of subjective analyses of temperature time series obtained from thermocouple-based temperature measurements also made at the tower sites (Clements et al. 2007; Heilman et al. 2015). Although period intervals could have also been delineated on the basis of when near-surface or higher-level wind-velocity components measured by the sonic anemometers departed substantially from ambient conditions, that option was not chosen because of the difficulty in isolating fire-induced velocity variations from ambient velocity variations, particularly at the beginning and ending of potential FFP periods. Following the procedure of Seto et al. (2013), perturbation velocities and temperatures during the defined FFP periods were computed using the mean velocities and temperatures obtained during the pre-FFP periods to allow for a better representation of the actual fire-induced velocity and temperature departures from the ambient state during the FFP periods. Finally, the resulting perturbation velocities and temperatures were used to compute instantaneous kinematic vertical turbulent momentum-flux $s'w'$ and heat-flux $w't'$ values, which form the basis for the sweep–ejection analyses described in the next section.

c. Sweep–ejection analyses

The assessment of the sweep–ejection dynamics that occurred during the TX2006, NJ2011, and NJ2012 fires utilized the well-known quadrant analysis technique as described, for example, in Wallace et al. (1972), Baldocchi and Meyers (1988), Katul et al. (1997, 2006), and Wallace (2016). Depending on the signs of the instantaneous perturbation streamwise velocities s', vertical velocities w', and temperatures t', the turbulent heat and momentum fluxes can be partitioned into instantaneous ejection, sweep, outward interaction, and inward interaction events. For turbulent heat fluxes, these events and associated quadrant designations are defined as follows:

ejections ($w't' > 0$): $w' > 0$ and $t' > 0$ (quadrant 1);
sweeps ($w't' > 0$): $w' < 0$ and $t' < 0$ (quadrant 3);
outward interactions ($w't' < 0$): $w' > 0$ and $t' < 0$ (quadrant 4); and
inward interactions ($w't' < 0$): $w' < 0$ and $t' > 0$ (quadrant 2),

where ejections represent upward fluxes of warm air, sweeps represent downward fluxes of cool air, outward interactions represent upward fluxes of cool air, and inward interactions represent downward fluxes of warm air. For turbulent momentum fluxes, the corresponding designations are as follows:

ejections ($s'w' < 0$): $s' < 0$ and $w' > 0$ (quadrant 4);
sweeps ($s'w' < 0$): $s' > 0$ and $w' < 0$ (quadrant 2);
outward interactions ($s'w' > 0$): $s' > 0$ and $w' > 0$ (quadrant 1); and
inward interactions ($s'w' > 0$): $s' < 0$ and $w' < 0$ (quadrant 3),

where ejections represent upward fluxes of low horizontal momentum air, sweeps represent downward fluxes of high horizontal momentum air, outward interactions represent upward fluxes of high horizontal momentum air, and inward interactions represent downward fluxes of low horizontal momentum air.

Occurrences of each type of event within the defined pre-FFP, FFP, and post-FFP periods at each monitoring level were counted for each experiment. Then, following the procedure of Katul et al. (1997), temporal means of the heat and momentum fluxes associated with ejection, sweep, outward interaction, and inward interaction events, given by

$$(\overline{w't'})_{Q,P} = \frac{1}{T_P}\int_0^{T_P} w'(\tau)t'(\tau)I_Q\, d\tau \quad \text{and} \tag{2}$$

$$(\overline{s't'})_{Q,P} = \frac{1}{T_P}\int_0^{T_P} s'(\tau)w'(\tau)I_Q\, d\tau, \tag{3}$$

were computed for the pre-FFP, FFP, and post-FFP periods at each monitoring level. In Eqs. (2) and (3), Q is the quadrant designation (Q = 1, 2, 3, or 4) associated with ejection, sweep, outward interaction, or inward interaction events; P is the period designation (pre-FFP, FFP, or post-FFP), T_P is the duration of the period; τ is time; and I_Q is a quadrant indicator function with a value of 1 when the instantaneous heat- and momentum-flux events [$w'(\tau)t'(\tau)$; $s'(\tau)w'(\tau)$] at time τ occur within quadrant Q, and a value of 0 otherwise. Note that the overall temporal means of the heat and momentum fluxes due to all of the individual ejection, sweep, outward interaction, and inward interaction events (i.e., flux contributions from all quadrants) during each period (pre-FFP, FFP, post-FFP) is simply the sum of the quadrant-specific heat- and momentum-flux temporal means, respectively:

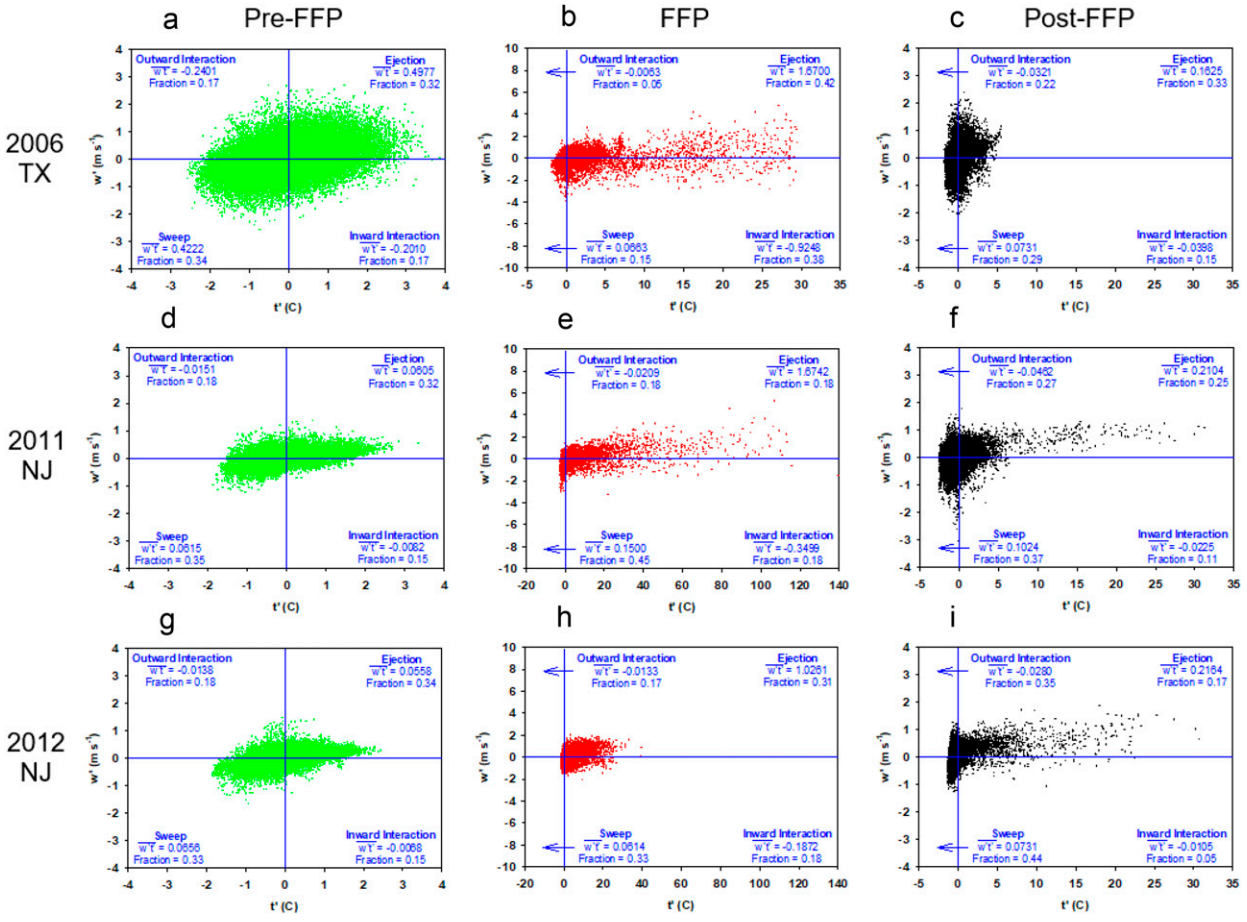

FIG. 1. Turbulent heat-flux quadrant scatterplots of outward interaction, ejection, inward interaction, and sweep events from sonic anemometer measurements of vertical velocity w' and temperature t' perturbations during (a)–(c) the TX2006 experiment (20 Hz, 2.1 m AGL, and $z/h_g = 1.4$), (d)–(f) the NJ2011 experiment (10 Hz, 3.0 m AGL, $z/h_u = 3$, and $z/h_o = 0.15$), and (g)–(i) the NJ2012 experiment (10 Hz, 3.0 m AGL, $z/h_u = 4.3$, and $z/h_o = 0.15$) showing event occurrences during the specified (left) pre-FFP, (center) FFP, and (right) post-FFP periods. The mean vertical heat-flux contribution and the fraction of the total number of events within each event quadrant are also noted.

$$(\overline{w't'})_P = \sum_{Q=1}^{4} (\overline{w't'})_{Q,P} \quad \text{and} \tag{4}$$

$$(\overline{s'w'})_P = \sum_{Q=1}^{4} (\overline{s'w'})_{Q,P}. \tag{5}$$

From these calculations and statistics, the relative importance of ejections, sweeps, outward interactions, and inward interactions in contributing to overall turbulent heat and momentum fluxes before, during, and after FFP for the TX2006, NJ2011, and NJ2012 experiments was assessed.

3. Results and discussion

a. Heat-flux sweep–ejection dynamics

Quadrant plots of the high-frequency instantaneous vertical turbulent heat fluxes measured during the defined pre-FFP, FFP, and post-FFP periods for the TX2006, NJ2011, and NJ2012 experiments were generated, and results for the lowest monitoring levels (2.1 or 3 m AGL) are shown in Fig. 1. The pre-FFP plots (Figs. 1a,d,g) clearly show the prominent roles sweep and ejection events play in redistributing heat vertically under daytime ambient conditions (i.e., no fire present), with the general tilting of the scatterplot footprint axes into the ejection and sweep quadrants. Sweep and ejection events comprised more than 60% of all events during the pre-FFP periods at the lowest monitoring levels, contributing to positive vertical turbulent heat fluxes via the upward flux of warm air (ejections) or the downward flux of cool air (sweeps). During the FFP periods (Figs. 1b,e,h), large positive temperature perturbations resulted in numerous large ejection and inward interaction (i.e., downward flux of warm air) events. The post-FFP periods during the NJ2011 and NJ2012 understory fire experiments (Figs. 1f,i) when smoldering occurred were also characterized by numerous relatively large ejection events, with positive temperature and vertical velocity perturbations near the surface still prominent and likely associated with the smoldering. Relatively large ejection events near the surface

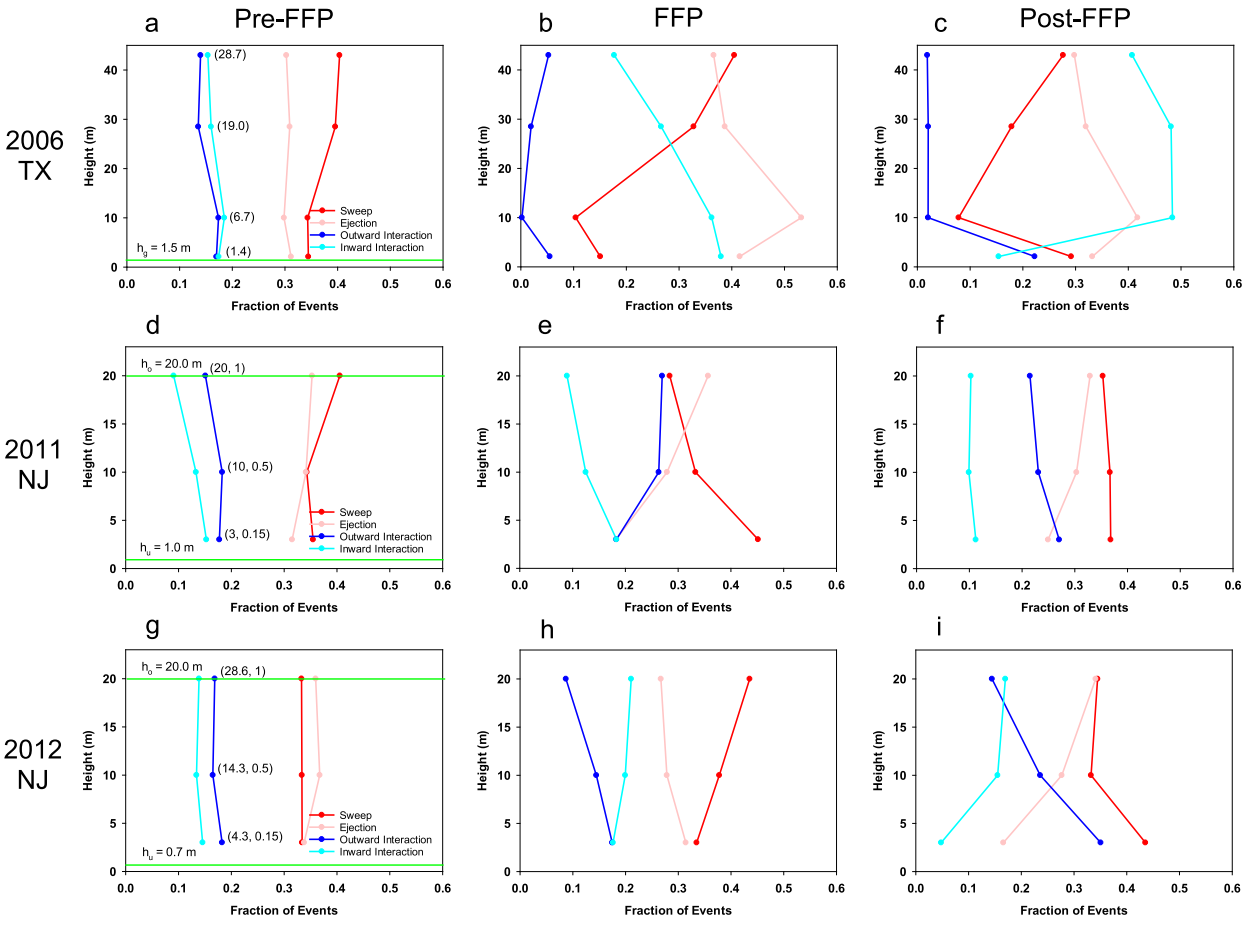

FIG. 2. Vertical profiles of the fractional number of sweep, ejection, outward interaction, and inward interaction events for turbulent heat fluxes during (a)–(c) the TX2006 experiment, (d)–(f) the NJ2011 experiment, and (g)–(i) the NJ2012 experiment showing profiles during the specified (left) pre-FFP, (center) FFP, and (right) post-FFP periods. In (a), (d), and (g), green lines indicate average grass height h_g, average understory vegetation height h_u, or average overstory vegetation height h_o and numbers in parentheses represent the (z/h_g) [in (a)] and (z/h_u, z/h_o) relative heights [in (d) and (g)] of the profile data points.

during the post-FFP smoldering period for the TX2006 grass-fire experiment did not occur (Fig. 1c). At upper levels, the quadrant plots for all periods (not shown) revealed even greater tilting of the scatterplot footprint axes into the ejection and sweep quadrants, consistent with the occurrence of stronger vertical velocity perturbations at higher levels above the surface.

For the TX2006 grass-fire experiment, heat-flux sweep and ejection events accounted for 60%–70% of all events during the pre-FFP period from the near-surface 2.1-m level (z/h_g = 1.4) up to the 43-m level (z/h_g = 28.7), with sweep events the most frequent (Fig. 2a). Both outward (upward flux of cool air) and inward (downward flux of warm air) interaction events occurred less than 20% of the time during the TX2006 pre-FFP period at all levels. For the NJ2011 and NJ2012 understory fire experiments, similar pre-FFP event-frequency profiles were found (Figs. 2d,g), although ejection events were actually the most frequent type of event during the 2012 experiment. Inward interaction events were the least frequent type of event for both New Jersey experiments.

While the pre-FFP periods for the TX2006 grass and NJ2011/NJ2012 forest-overstory vegetation environments were characterized by similar event-frequency profiles, the profiles for the two different types of environments changed dramatically in the presence of advancing line fires. During the FFP period for the TX2006 grass-fire experiment, ejection events became the most common type of event primarily at the expense of sweep events (Fig. 2b). Inward interaction event frequencies also increased substantially at lower levels on the tower. In comparison with TX2006, very different event-frequency profiles were present during the FFP periods for the NJ2011/NJ2012 experiments (Figs. 2e,h). Sweep-event frequencies for NJ2011 increased dramatically near the surface (3 m AGL, z/h_u = 3, and z/h_o = 0.15) at the expense of ejection events. Sweep events were also the most frequent type of event during the NJ2012 experiment, with frequencies increasing with height generally at the expense of ejection events. These differences between the grass-fire and understory-fire event profiles suggest that the presence of overstory vegetation during wildland fires may further promote the occurrence of heat-flux sweep events above surface fire fronts in the h_u–h_o layer, whereas wildland fires in grass environments with no

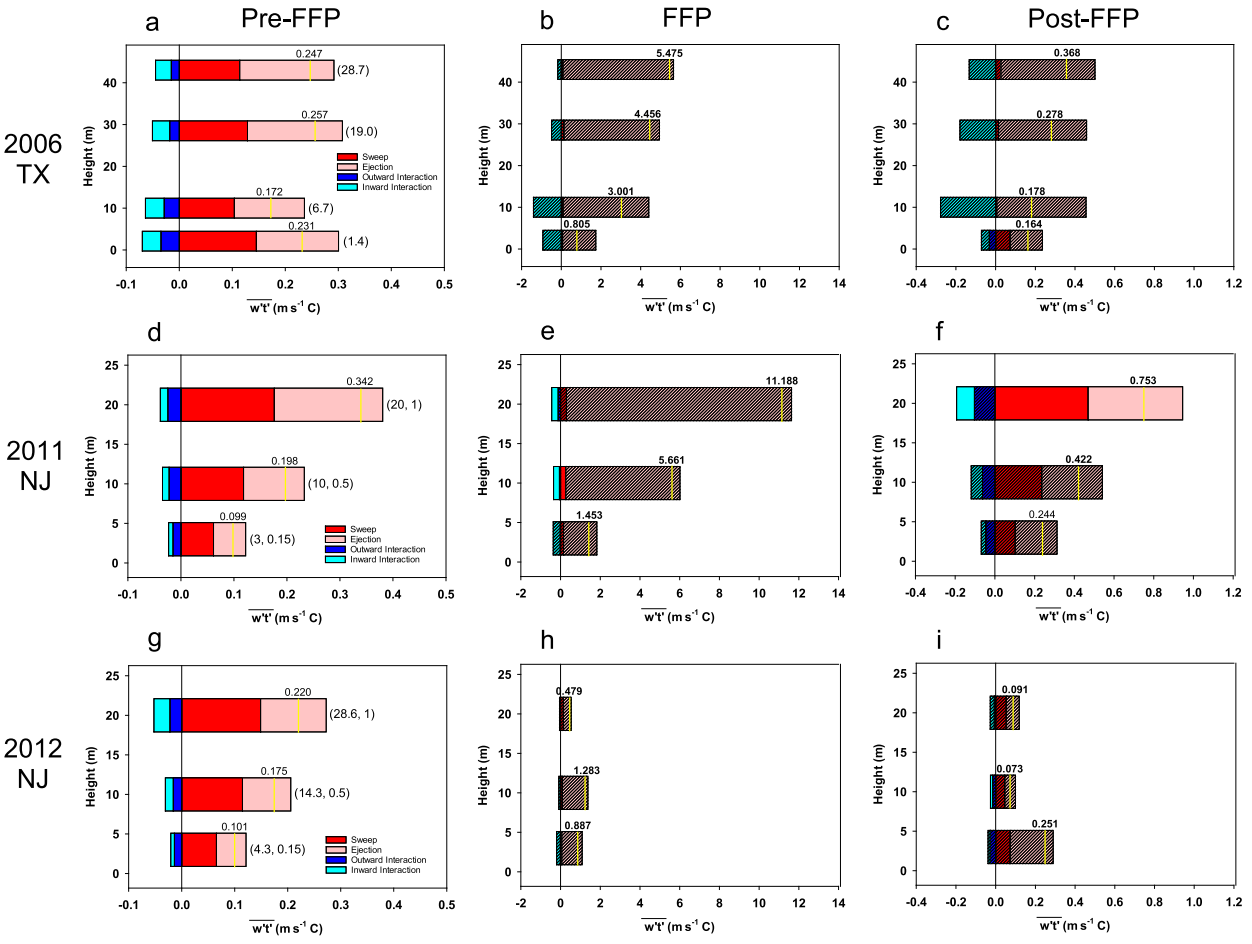

FIG. 3. Event contributions to the mean turbulent heat fluxes within the (left) pre-FFP, (center) FFP, and (right) post-FFP periods from sweep, ejection, outward interaction, and inward interaction events at different height levels during (a)–(c) the TX2006 experiment, (d)–(f) the NJ2011 experiment, and (g)–(i) the NJ2012 experiment. Striped bars indicate statistically significant variations ($p < 0.01$) from the pre-FFP contributions for each type of event. The mean vertical turbulent heat flux at each height level resulting from the four different event contributions is depicted by the yellow vertical lines and associated numerical values (m s^{-1} C) above the lines; boldface numbers indicate statistically significant variations ($p < 0.01$) from the pre-FPP mean values. Numbers in parentheses represent the (z/h_g) [in (a)] and (z/h_u, z/h_o) [in (d) and (g)] relative heights of the contribution data.

overstory vegetation present can potentially lead to ejection-event dominated vertical heat-flux regimes above surface fire fronts and above h_g. Caution in attributing the differences in the observed event profiles solely to the presence or absence of forest overstory vegetation is warranted, however, because fire intensity and backing versus heading fire considerations are factors.

The post-FFP periods also demonstrated marked differences in event-frequency profiles between the grass and overstory dominated vegetation environments (Figs. 2c,f,i). Inward interaction event frequencies at heights above 2.1 m increased even further than what was observed during the FFP period, while ejection-event and sweep-event frequencies remained relatively large and small at the 10-m level, respectively, following FFP for the TX2006 grass-fire experiment. In contrast, the post-FFP periods during the NJ2011/NJ2012 understory fire experiments continued to exhibit mainly sweeps, with outward interactions quite prominent as well near the smoldering surface during NJ2012.

The turbulent heat-flux event frequencies highlighted in Fig. 2 only tell part of the sweep–ejection dynamics story. Actual contributions of the different types of events to the mean vertical turbulent heat fluxes that occurred during the pre-FFP, FFP, and post-FFP periods were also examined and are shown in Fig. 3. Ejection- and sweep-event contribution values were similar and dominated the outward and inward interaction-event contributions at all height levels in the pre-FFP periods for all experiments (Figs. 3a,d,g). Ejection-event contributions were slightly larger than the sweep-event contributions at all tower levels for TX2006, even though sweep events were more prevalent (Fig. 2a). The resulting mean heat-flux values during the pre-FFP periods (see yellow vertical bars in Fig. 3) clearly increased with height within the forest overstory vegetation layers for the NJ2011/NJ2012 experiments (Figs. 3d,g), but no such vertical trend was evident above the grass environment for the TX2006 experiment (Fig. 3a).

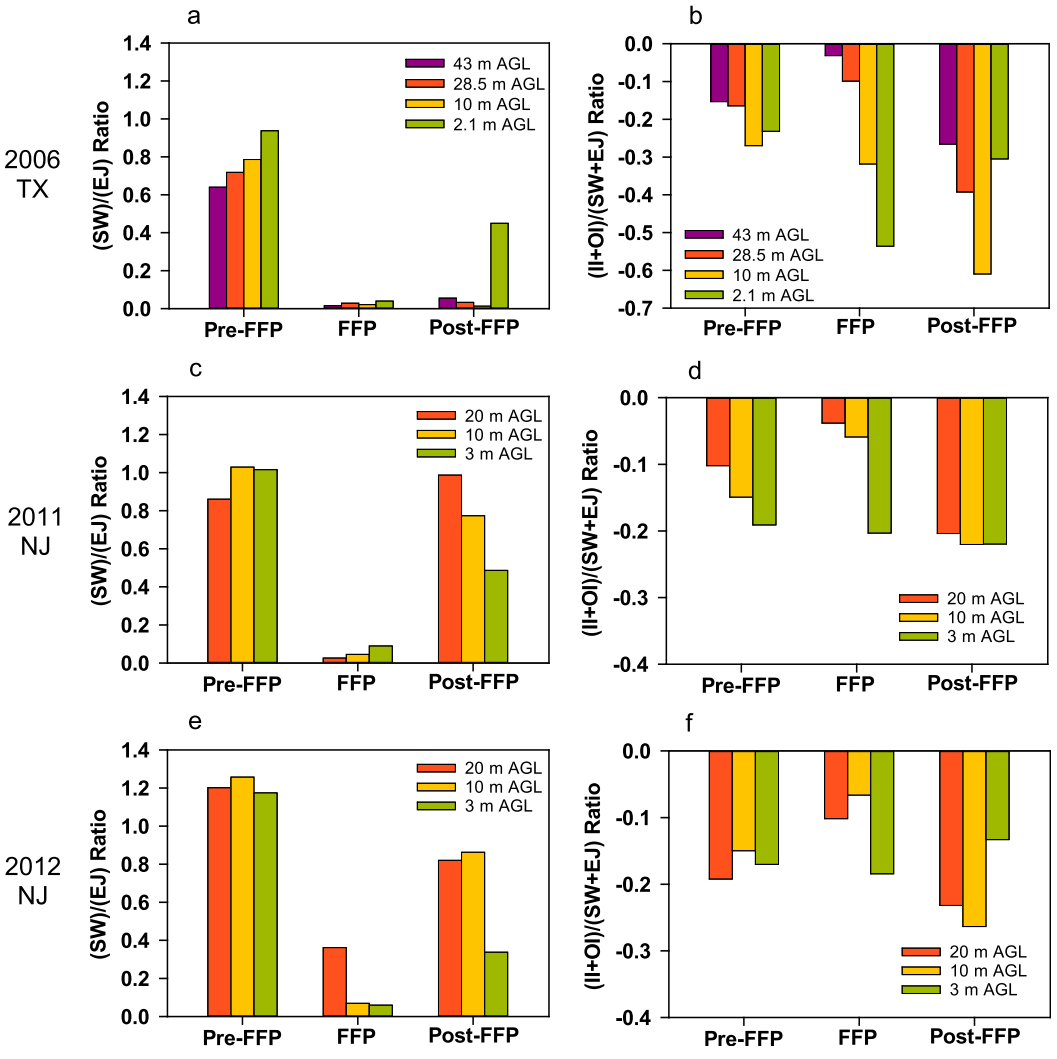

FIG. 4. Ratios of the (left) contributions of sweeps (SW) vs ejections (EJ) and (right) contributions of inward interactions (II) + outward interactions (OI) vs SW + EJ to the mean turbulent heat fluxes at different height levels during the pre-FFP, FFP, and post-FFP periods for (a),(b) the TX2006 experiment; (c),(d) the NJ2011 experiment; and (e),(f) the NJ2012 experiment.

During the FFP periods for both the grass-fire and understory-fire experiments, the contributions from ejections to the mean vertical turbulent heat-flux values at all vertical levels completely dominated the contributions from sweeps, outward interactions, and inward interactions (Figs. 3b,e,h), even though the previously discussed FFP event-frequency profiles in Figs. 2b, 2e and 2h indicate the number of sweep events sometimes exceeded ejection events. Ejection contributions continued to dominate during the post-FFP period for the TX2006 grass-fire experiment (Fig. 3c), whereas sweep and ejection contributions were more similar to each other during the post-FFP periods for the NJ2011/NJ2012 understory fire experiments (Figs. 3f,i) as they were during the pre-FFP periods. It is worth noting that the ejection, sweep, outward interaction, and inward interaction contributions to the mean heat fluxes during the FFP and post-FFP periods for NJ2012 resulted in the largest mean heat-flux values occurring either near the surface (3 m AGL, $z/h_u = 4.3$, and $z/h_o = 0.15$) or at the midcanopy level (10 m AGL, $z/h_u = 14.3$, and $z/h_o = 0.5$). This is in contrast to the TX2006 and the NJ2011 experiments, when mean heat-flux values generally increased with height above the surface, and is likely due to the very low line-fire intensity in the 2012 understory fire experiment. As shown in Fig. 3, most of the differences in the FFP and post-FFP mean heat fluxes and event contributions at each height level relative to the pre-FFP mean heat fluxes and contributions at the same height level were statistically significant ($p < 0.01$), from a Kruskal–Wallis one-way analysis of variance (ANOVA) on ranks assessment (appropriate for nonnormal distributions).

The relative contributions of the different event types to the overall mean heat fluxes during the pre-FFP, FFP, and post-FFP periods are further summarized in Fig. 4. Ratios of the

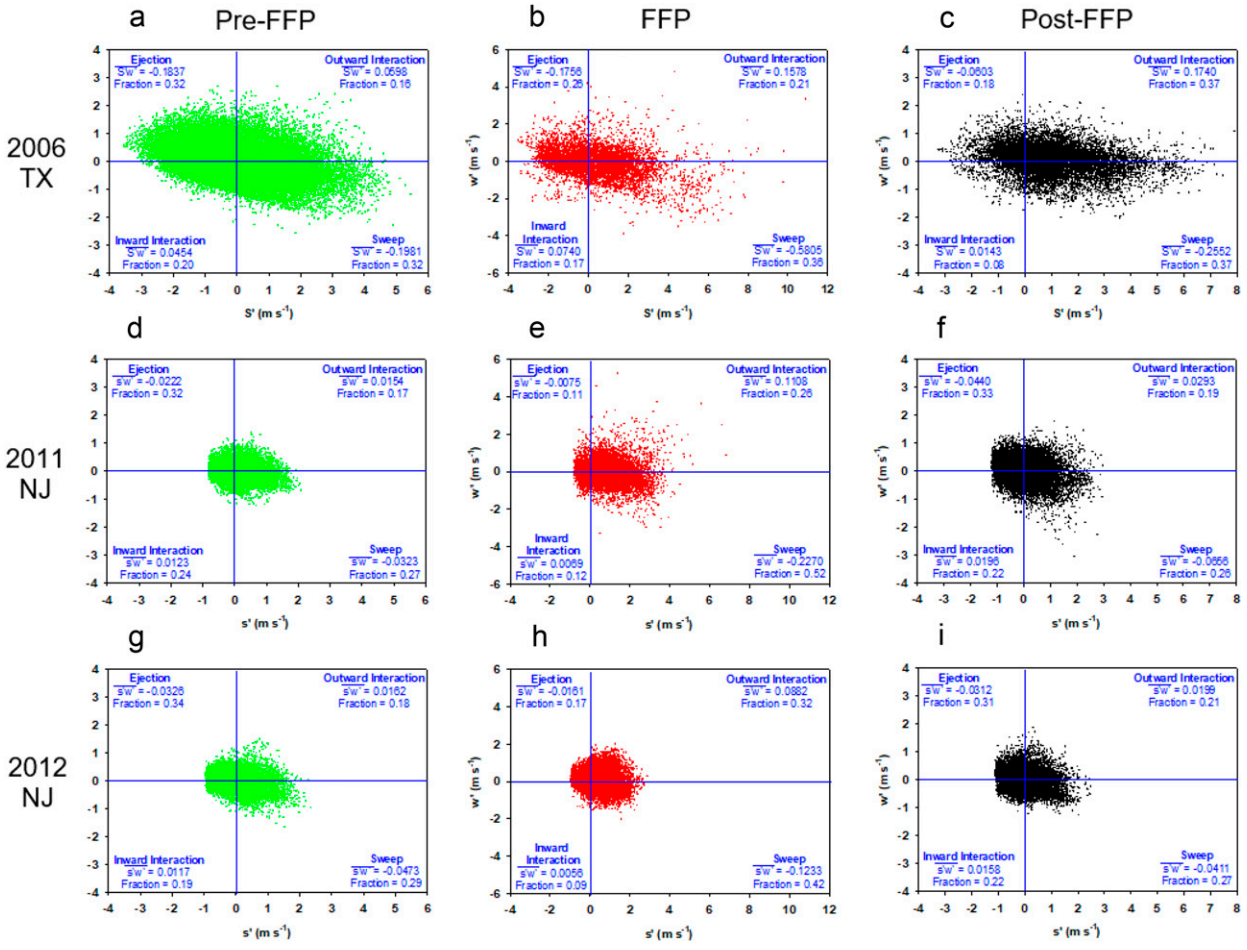

FIG. 5. As in Fig. 1, but for turbulent momentum-flux quadrant scatterplots of ejection, outward interaction, sweep, and inward interaction events from sonic anemometer measurements of w' and horizontal streamwise velocity s' perturbations.

sweep to ejection contributions (Figs. 4a,c,e) and ratios of the outward interaction plus inward interaction contributions to the sweep plus ejection contributions (Figs. 4b,d,f) highlight the sweep–ejection dynamics regime changes associated with turbulent heat fluxes that can occur when wildland fires are present. The Fig. 4 summaries suggest it is the sweep–ejection contribution ratios that undergo the most profound changes when wildland fires are present, with fire periods being characterized as ejection-dominated environments for heat fluxes as opposed to the sweep- and ejection-dominated environments when no fires are present. Furthermore, for higher-intensity head fires when no forest overstory vegetation is present, the ejection-dominated environment during FFP periods may very well linger into the smoldering post-FFP periods (particularly at higher levels above the surface), as shown in Fig. 4a. The summary plots comparing outward plus inward interaction contributions to sweep plus ejection contributions (Figs. 4b,d,f) suggest that changes in the relative contributions of outward and inward interactions versus sweeps and ejections due to the presence of surface fires may be less pronounced than the sweep versus ejection contribution changes. Note, however, that consistent decreases in ratio magnitudes during the FFP periods (Figs. 4b,d,f) were observed at higher levels on the towers for all three experiments.

b. *Momentum-flux sweep–ejection dynamics*

Similar to the sweep–ejection dynamics analyses for turbulent heat fluxes, analyses of the sweep–ejection dynamics governing the vertical turbulent fluxes of horizontal momentum for the three fire experiments were carried out. Example quadrant plots showing the instantaneous high-frequency (10 or 20 Hz) near-surface (2.1 or 3 m AGL) vertical fluxes of horizontal momentum during the pre-FFP, FFP, and post-FFP periods for the three fire experiments are shown in Fig. 5. Note that for momentum-fluxes, ejection (upward flux of low horizontal momentum air) and sweep (downward flux of high horizontal momentum air) events lead to negative vertical momentum fluxes while outward (upward flux of high horizontal momentum air) and inward (downward flux of low horizontal momentum air) interaction events lead to positive vertical momentum fluxes. Ejection and sweep events played a more prominent role in vertically redistributing horizontal momentum than outward and inward interaction events during the pre-FFP periods for all experiments, as inferred from the

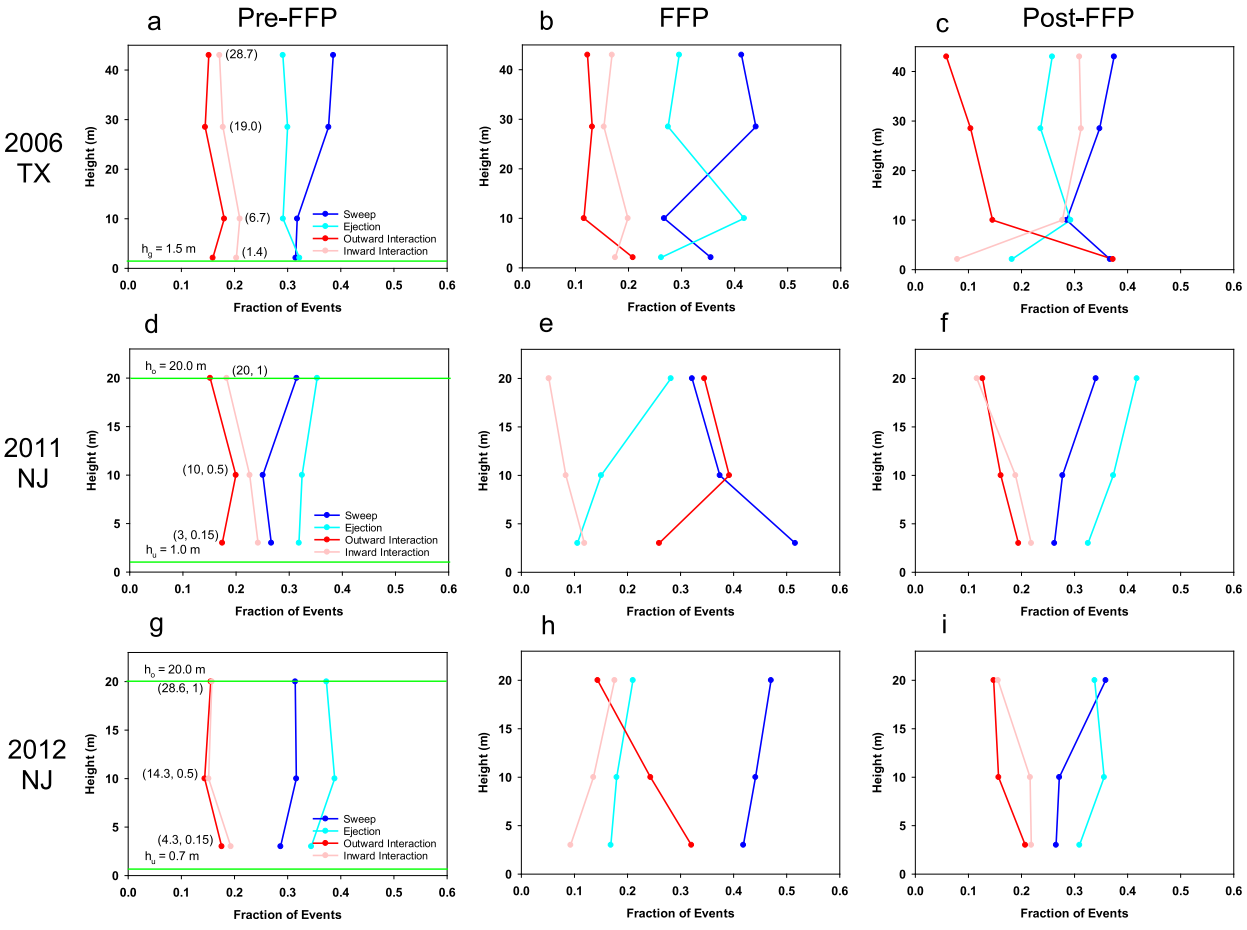

FIG. 6. As in Fig. 2, but for turbulent momentum fluxes.

slight tilting of the scatterplot footprint axes into the ejection and sweep quadrants (Figs. 5a,d,g). The tilting of the footprint axes into the ejection and sweep quadrants was also evident and generally more pronounced at higher levels above the surface for all experiments (figures not shown), as was the case for the turbulent heat-flux analyses. There were also more frequent occurrences of stronger magnitude events at higher levels above the ground in all the pre-FFP event quadrants, as velocity perturbations typically tend to increase above the surface in the ABL.

With the passage of fire fronts through the monitoring site locations, there were numerous occurrences of relatively large positive horizontal streamwise velocity perturbations concurrently with relatively large positive and negative vertical velocity perturbations at the lowest monitoring levels (Figs. 5b,e,h), an indication that FFP periods can be conducive to strong outward interaction (upward flux of high horizontal momentum air) and sweep (downward flux of high horizontal momentum air) events near the surface and immediately above surface fire fronts. During the post-FFP periods, occurrences of relatively strong outward interaction and sweep events near the surface were still noted (Figs. 5c,f,i), but to a lesser degree than during the FFP periods. At higher levels, there were more frequent occurrences of stronger magnitude events as was observed during the pre-FFP periods.

A closer examination of the actual number of occurrences of momentum-flux ejection, sweep, outward interaction, and inward interaction events at different height levels for the three experiments revealed substantial variations among the experiments. Vertical profiles of pre-FFP event frequencies during the TX2006 grass-fire experiment indicate both sweep and ejection events occurred more often than outward and inward interaction events, with sweep events being the most frequent at all height levels except at the 2.1-m level (z/h_g = 1.4) (Fig. 6a). This is in contrast to the pre-FFP event-frequency profiles for the NJ2011/NJ2012 understory-fire experiments, where ejection events occurred more often than any other event at all height levels from above the understory vegetation to near the top of the canopy (Figs. 6d,g). These findings suggest the presence or absence of forest overstory vegetation may have had an impact on whether sweeps or ejections were the most frequent type of event in the nonfire periods, a result consistent with many previous studies of sweep–ejection dynamics in nonfire environments (e.g., Baldocchi and Meyers 1988; Katul et al. 1997, 2006; Poggi et al. 2004).

Differences in momentum-flux event-frequency profiles between the experiments were even more pronounced during the FFP periods (Figs. 6b,e,h). The absence of forest overstory vegetation for the TX2006 experiment may have been conducive

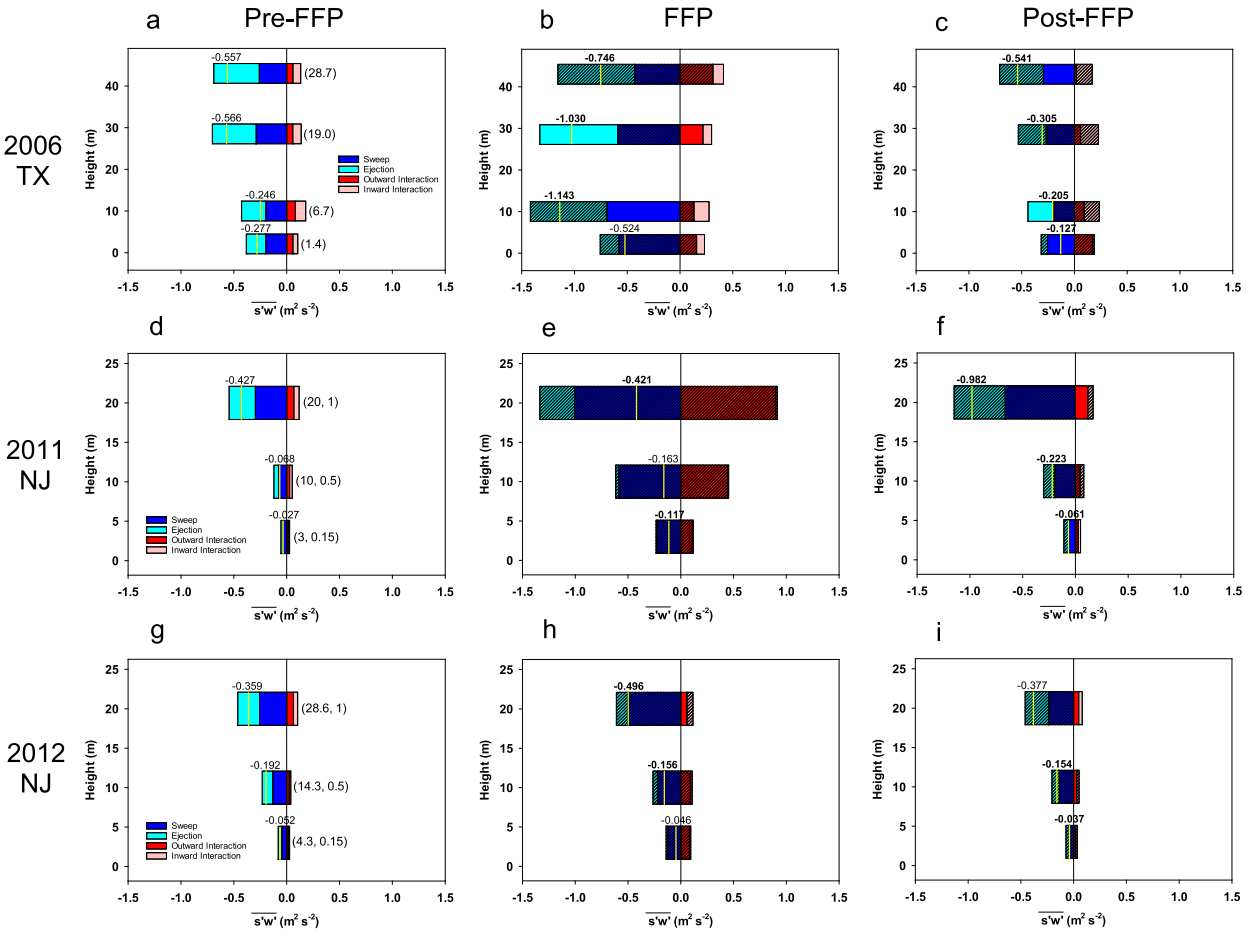

FIG. 7. As in Fig. 3, but for turbulent momentum fluxes. The numerical values associated with the yellow vertical lines are in meters squared per second squared.

to sweeps and ejections continuing their prevalence at all height levels during the FFP period (Fig. 6b), with ejection-event occurrences exceeding sweep occurrences at the 10-m level (z/h_g = 6.7) instead of the 2.1-m level (z/h_g = 1.4), as was the case during the pre-FFP period. For the NJ2011/NJ2012 understory fire experiments, ejection-event frequencies diminished substantially from what was observed during the pre-FFP period (Figs. 6e,h), while sweep events generally occurred more frequently. The presence of surface burning beneath the forest overstory vegetation also increased the frequency of occurrence of outward interactions to the extent that they were actually the most frequent type of event at the 10-m (z/h_u = 10; z/h_o = 0.5) and 20-m (z/h_u = 20; z/h_o = 1) levels for NJ2011 (Fig. 6e).

The post-FFP periods for the grass-fire and understory-fire experiments were also quite different in their event-frequency profiles (Figs. 6c,f,i). Ejections and sweeps returned to their dominance in occurrence for the NJ2011/NJ2012 understory-fire experiments (Figs. 6f,i), whereas increases in outward and inward interaction occurrences from what was observed during the pre-FFP and FFP periods characterized the 2.1-m (z/h_g = 1.4) level and the 10–43-m (6.7 $\leq z/h_g \leq$ 28.7) layer, respectively, for the TX2006 grass-fire experiment (Fig. 6c).

The actual contributions of the different types of events to the mean turbulent momentum fluxes during each period for the three experiments are summarized in Fig. 7. Even though sweep events were the most prevalent type of event at most levels during the pre-FFP period for TX2006, ejection events usually contributed more to the overall negative momentum fluxes characterizing each level (Fig. 7a), and the relative contributions of ejections compared to sweeps increased with height during the pre-FFP period. The relative sweep–ejection contribution behavior for momentum fluxes during the pre-FFP periods for the NJ2011/NJ2012 understory-fire experiments was quite different; sweep contributions exceeded ejection contributions at all height levels (Figs. 7d,g). The combined influence of all four event types during the pre-FFP periods resulted in mean momentum fluxes (noted by yellow vertical lines in Fig. 7) clearly increasing with height for NJ2011/NJ2012 (Figs. 7d,g) but less consistent increases with height for TX2006 (Fig. 7a).

During the FFP periods, differences in momentum-flux contributions between sweeps and ejections increased significantly for the NJ2011/NJ2012 understory-fire experiments, with sweep contributions completely dominating the ejection

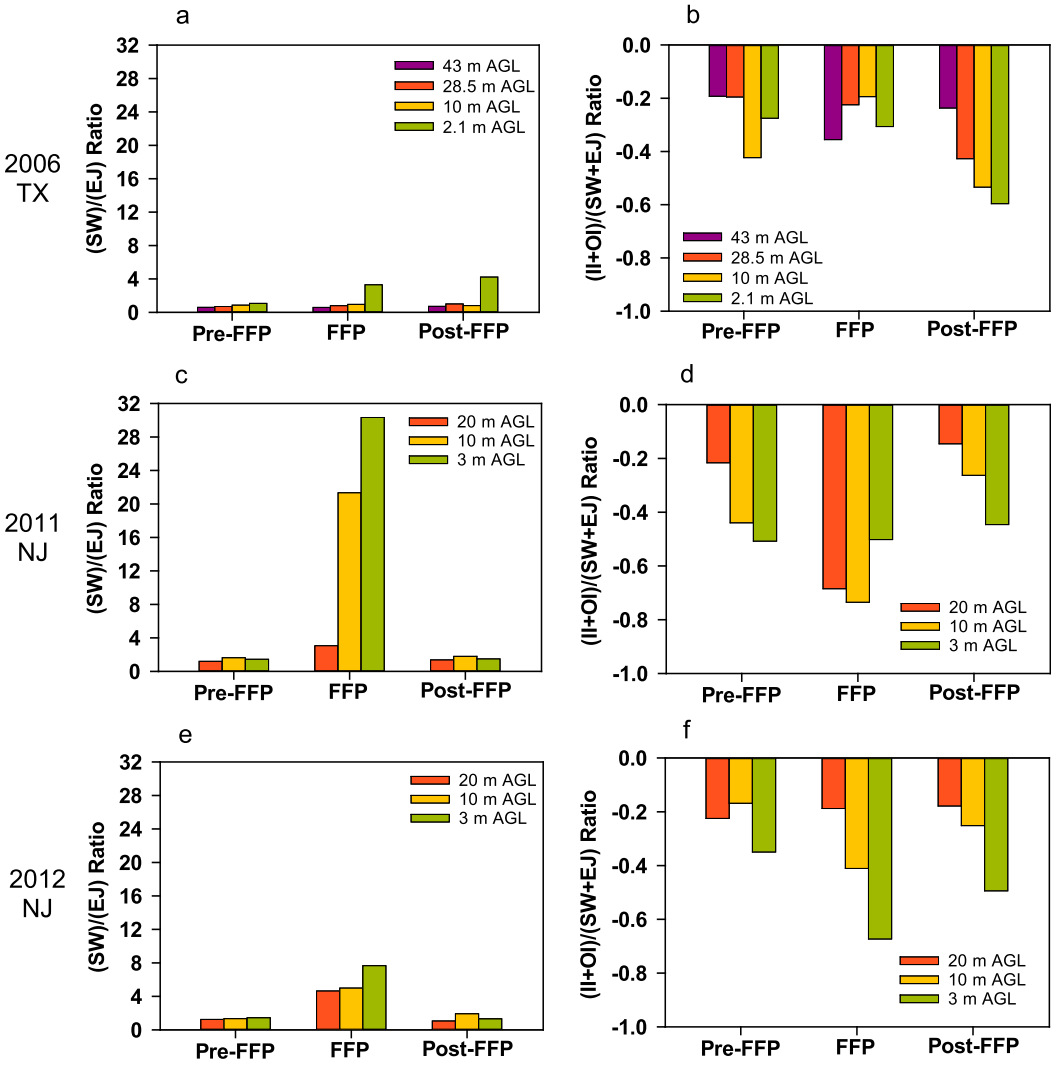

FIG. 8. As in Fig. 4, but for turbulent momentum fluxes.

contributions at all height levels (Figs. 7e,h). In contrast, ejection and sweep contributions remained quite similar in the 10–43-m ($6.7 \leq z/h_g \leq 28.7$) layer for the TX2006 grass-fire experiment (Fig. 7b); only at the near-surface 2.1-m ($z/h_g = 1.4$) level did sweep contributions dominate. Another conspicuous feature of the FFP periods was the prominent role outward interactions played in contributing to the mean momentum fluxes for the understory fires, especially during NJ2011 (Fig. 7e). The strong outward interaction contributions (positive momentum flux) substantially offset the negative momentum-flux contributions associated with sweeps at all levels, and this greatly diminished the overall mean momentum-flux magnitudes (yellow vertical lines in Figs. 7e and 7h). As with the turbulent heat fluxes, most of the differences in the overall mean momentum fluxes and event contribution magnitudes between the pre-FFP and FFP periods were statistically significant ($p < 0.01$; Kruskal–Wallis ANOVA on ranks assessment). After the FFP periods, event-contribution behavior for all the experiments transitioned to behavior more like what was observed during their respective pre-FFP periods (Figs. 7c,f,i), although many of the pre-FFP versus post-FFP contribution differences remained statistically significant.

Figure 8 summarizes the relative importance of all the different event types in contributing to the overall vertical momentum-flux fields for the three experiments. Comparing sweep contributions to ejection contributions (Figs. 8a,c,e), it is clear that the presence of surface fire fronts beneath forest overstory vegetation tended to substantially increase the sweep to ejection contribution ratios, particularly at lower height levels. Increases were smaller or nonexistent at the different height levels for the grass-fire experiment. Maximum ratios during the FFP periods ranged from 3.3 at the 2.1-m level ($z/h_g = 1.4$) for TX2006 to 30.3 at the 3-m level ($z/h_u = 3$; $z/h_o = 0.15$) for the NJ2011. Ratio values ranging from 0.60 to 1.01 were observed at all levels except the 2.1-m level during the pre-FFP and post-FFP periods for TX2006, highlighting the relative importance that ejections played in the vertical turbulent transport of horizontal momentum with no fire present.

This contrasts with the observed pre-FFP and post-FFP ratios for the understory-fire experiments when sweep contributions exceeded ejection contributions, with ratios exceeding one at all height levels.

The inward interaction + outward interaction versus sweep + ejection ratio (also referred to as exuberance Shaw et al. 1983) plots shown in Figs. 8b, 8d and 8f reveal inconsistent changes moving from the pre-FFP periods to the post-FFP periods. Ratio magnitudes were larger during the FFP periods than during the pre and post-FFP periods at most height levels for the NJ2011/NJ2012 understory-fire experiments. This was not the case for the TX2006 grass-fire experiment, as ratio magnitudes at most of the height levels were at a maximum during the post-FFP period.

4. Summary and conclusions

Recent wildland fire experiments in grassland and forested environments have expanded our understanding of the potential impacts that wildland fires can have on atmospheric boundary layer turbulence regimes and their feedback on fire behavior and smoke dispersion. This study focused on extending the previous turbulence analyses presented in Clements et al. (2008) and Heilman et al. (2015, 2017, 2019) for three experimental wildland fires (one grassland fire; two understory fires) that occurred in Texas and New Jersey in 2006, 2011, and 2012. Specifically, tower-based high-frequency (10 or 20 Hz) wind and temperature measurements made in the vicinity of the fire fronts for each experiment were used to assess differences in frequencies of occurrence of sweep, ejection, outward interaction, and inward interaction events and differences in their contributions to vertical turbulent heat and momentum fluxes before, during, and after the passage of fire fronts in the grassland and forested environments.

The analyses indicate that the presence of surface fire fronts can substantially change the sweep–ejection dynamics for turbulent heat and momentum fluxes that typically occur in grassland and forested environments under no-fire conditions. While occurrences of sweep and ejection events for heat and momentum fluxes were found to be substantially more frequent than outward and inward interaction events during pre-FFP periods in both environments (a finding consistent with previous studies under no-fire conditions; e.g., Baldocchi and Meyers 1988; Katul et al. 1997), heat-flux inward interaction events (downward flux of warm air from above) and momentum-flux outward interaction events (upward flux of high horizontal momentum air from below) tended to be more frequent during FFP periods in the grassland and forested environments, respectively. After the passage of fire fronts, departures of event frequencies from the observed pre-FFP frequencies were also noted. Inward interaction events contributing to the downward flux of warm air from above were relatively frequent in the post-FFP grass-fire environment; no such behavior was observed in the post-FFP understory-fire environment. Momentum-flux inward interaction events contributing to the downward flux of low-momentum air from above and momentum-flux outward interaction events contributing to the upward flux of high-momentum air from below were relatively frequent at numerous heights in the post-FFP grass-fire environment. Again, no such behavior was observed in the post-FFP understory-fire environment.

The observed actual contributions of individual sweep, ejection, outward interaction, and inward interaction events at their different frequencies of occurrence to the mean turbulent heat and momentum fluxes during the pre-FFP, FFP, and post-FFP periods underscore the significant impacts that surface fires can have on the vertical redistribution of heat and momentum due to turbulence. In contrast to no-fire grassland and forested environments where previous observations have shown that sweeps and ejections together make the largest contributions to vertical fluxes of heat and momentum in the lower boundary layer (e.g., Baldocchi and Meyers 1988; Katul et al. 1997), results from this study suggest that surface fires can lead to 1) heat-flux contributions from ejections completely dominating other mechanisms, and 2) momentum-flux contributions from outward interactions (upward flux of high horizontal momentum air from below) sometimes substantially offsetting the contributions of sweeps and ejections. Furthermore, the presence of wildland fires in grassland and forested environments tends to diminish the contributions of sweeps compared to ejections in determining mean vertical turbulent heat fluxes near the fires. For mean vertical turbulent momentum fluxes, wildland fires tend to enhance the contributions of sweeps compared to ejections, especially in forested environments and near the surface. This latter point highlights the potential importance of turbulent transfer of high momentum air from aloft into the combustion zones of wildland fires, even though the enhanced buoyancy above combustion zones might suggest the upward turbulent transfer of high momentum air away from combustion zones was dominant.

The event-frequency and contribution analyses performed in this study reveal that the presence or absence of overstory vegetation may have an impact on the manner in which heat and momentum are redistributed by turbulence above surface fire fronts. However, caution is warranted in attributing differences in the observed sweep–ejection dynamics entirely to overstory vegetation effects. The wildland fires considered in this study varied in intensity, their rates of spread, and the manner in which they spread in relation to the ambient winds (i.e., backing vs heading fires). Each of these factors along with the presence or absence of overstory vegetation very likely affected how turbulence was generated and dissipated in the vicinity of the fire fronts, which in turn affected the spatial and temporal characteristics of the sweeps, ejections, outward interactions, and inward interactions that occurred. Further field investigations of sweep–ejection dynamics during different types of wildland fire events in different types of vegetation environments are needed to close the knowledge gaps in our understanding of how fire-induced turbulence actually redistributes heat and momentum, and how that redistribution feeds back on fire behavior.

In addition to field investigations, sensitivity simulations of the responses of sweep–ejection dynamics to a range of fire and environmental variations utilizing high resolution coupled fire–atmosphere models [e.g., ‘‘FIRETEC’’ (Linn et al. 2002); WFDS (Mell et al. 2007); University of Utah’s Large-Scale

Eddy Simulation (UU-LES; Sun et al. 2009); WRF's coupled atmosphere wildland fire model (WRF-Fire; Coen et al. 2013)] are needed and would likely accelerate the closing of our current knowledge gaps. Many of these and other modeling tools have already been used to identify turbulence processes important for fire spread that are inherently related to or involved in sweep–ejection dynamics, including fire-induced vortices, fire-induced turbulent updrafts and downdrafts, and ambient and fire-induced convection within canopy layers (e.g., Linn and Cunningham 2005; Cunningham and Linn 2007; Pimont et al. 2009; Sun et al. 2009; Forthofer and Goodrick 2011; Mueller et al. 2014; Kiefer et al. 2015). Taking advantage of these modeling systems to more explicitly examine the spatial and temporal (periodicity) patterns of sweep, ejection, outward interaction, and inward interaction events near fire fronts and their impacts on fire-spread variability is an important next step.

Acknowledgments. Funding for this study was provided by the USDA Forest Service and the U.S. Joint Fire Science Program under Project 09-1-04-1. We thank the anonymous reviewers of this paper for their constructive and insightful comments.

Data availability statement. The observational datasets used in this study are available online from the USDA Forest Service Northern Research Station (http://eams2.usfs.msu.edu/outgoing/Heilman/2020_JAMC/2020_JAMC_Pub_data.tgz).

REFERENCES

Baldocchi, D. D., and B. A. Hutchison, 1987: Turbulence in an almond orchard: Vertical variation in turbulent statistics. *Bound.-Layer Meteor.*, **40**, 127–146, https://doi.org/10.1007/BF00140072.

——, and T. P. Meyers, 1988: Turbulence structure in a deciduous forest. *Bound.-Layer Meteor.*, **43**, 345–364, https://doi.org/10.1007/BF00121712.

Banerjee, T., F. De Roo, and M. Mauder, 2017: Connecting the failure of K theory inside and above vegetation canopies and ejection–sweep cycles by a large-eddy simulation. *J. Appl. Meteor. Climatol.*, **56**, 3119–3131, https://doi.org/10.1175/JAMC-D-16-0363.1.

Beer, T., 1991: The interaction of wind and fire. *Bound.-Layer Meteor.*, **54**, 287–308, https://doi.org/10.1007/BF00183958.

Bergström, H., and U. Högström, 1989: Turbulent exchange above a pine forest II: Organized structures. *Bound.-Layer Meteor.*, **49**, 231–263, https://doi.org/10.1007/BF00120972.

Charney, J. J., and Coauthors, 2019: Assessing forest canopy impacts on smoke concentrations using a coupled numerical model. *Atmosphere*, **10**, 273, https://doi.org/10.3390/atmos10050273.

Chen, F., 1990: Turbulent characteristics over a rough natural surface. Part I: Turbulent structures. *Bound.-Layer Meteor.*, **52**, 151–175, https://doi.org/10.1007/BF00123182.

Clements, C. B., 2007: Experimental studies of fire-atmosphere interactions during grass fires. Ph.D. dissertation, University of Houston, 142 pp.

——, and Coauthors, 2007: Observing the dynamics of wildland grass fires. *Bull. Amer. Meteor. Soc.*, **88**, 1369–1382, https://doi.org/10.1175/BAMS-88-9-1369.

——, S. Zhong, X. Bian, W. E. Heilman, and D. W. Byun, 2008: First observations of turbulence generated by grass fires. *J. Geophys. Res.*, **113**, D22102, https://doi.org/10.1029/2008JD010014.

Coen, J. L., M. Cameron, J. Michalakes, E. G. Patton, P. J. Riggan, and K. M. Yedinak, 2013: WRF-Fire: Coupled weather–wildland fire modeling with the Weather Research and Forecasting model. *J. Appl. Meteor. Climatol.*, **52**, 16–38, https://doi.org/10.1175/JAMC-D-12-023.1.

Cunningham, P., and R. R. Linn, 2007: Numerical simulations of grass fires using a coupled atmosphere-fire model: Dynamics of fire spread. *J. Geophys. Res.*, **112**, D05108, https://doi.org/10.1029/2006JD007638.

Finnigan, J. J., 1979: Turbulence in waving wheat. Part II. Structure of momentum transfer. *Bound.-Layer Meteor.*, **16**, 213–236, https://doi.org/10.1007/BF02350512.

——, 2000: Turbulence in plant canopies. *Annu. Rev. Fluid Mech.*, **32**, 519–571, https://doi.org/10.1146/annurev.fluid.32.1.519.

Forthofer, J. M., and S. L. Goodrick, 2011: Review of vortices in wildland fire. *J. Combust.*, **2011**, 1–14, https://doi.org/10.1155/2011/984363.

Heilman, W. E., S. Zhong, J. L. Hom, and J. J. Charney, 2013: Development of modeling tools for predicting smoke dispersion from low-intensity fires. U.S. Joint Fire Science Program Project 09-1-04-1 Final Rep., 65 pp., https://www.firescience.gov/projects/09-1-04-1/project/09-1-04-1_final_report.pdf.

——, C. B. Clements, D. Seto, X. Bian, K. L. Clark, N. S. Skowronski, and J. L. Hom, 2015: Observations of fire-induced turbulence regimes during low-intensity wildland fires in forested environments: Implications for smoke dispersion. *Atmos. Sci. Lett.*, **16**, 453–460, https://doi.org/10.1002/asl.581.

——, X. Bian, K. L. Clark, N. S. Skowronski, J. L. Hom, and M. R. Gallagher, 2017: Atmospheric turbulence observations in the vicinity of surface fires in forested environments. *J. Appl. Meteor. Climatol.*, **56**, 3133–3150, https://doi.org/10.1175/JAMC-D-17-0146.1.

——, ——, ——, and S. Zhong, 2019: Observations of turbulent heat and momentum fluxes during wildland fires in forested environments. *J. Appl. Meteor. Climatol.*, **58**, 813–829, https://doi.org/10.1175/JAMC-D-18-0199.1.

Katul, G., and J. D. Albertson, 1998: An investigation of higher-order closure models for a forested canopy. *Bound.-Layer Meteor.*, **89**, 47–74, https://doi.org/10.1023/A:1001509106381.

——, G. Kuhn, J. Schieldge, and C.-I. Hsieh, 1997: The ejection-sweep character of scalar fluxes in the unstable surface layer. *Bound.-Layer Meteor.*, **83** (1), 1–26, https://doi.org/10.1023/A:1000293516830.

——, D. Poggi, D. Cava, and J. Finnigan, 2006: The relative importance of ejections and sweeps to momentum transfer in the atmospheric boundary layer. *Bound.-Layer Meteor.*, **120**, 367–375, https://doi.org/10.1007/s10546-006-9064-6.

Kiefer, M. T., W. E. Heilman, S. Zhong, J. J. Charney, and X. Bian, 2015: Mean and turbulent flow downstream of a low-intensity fire: Influence of canopy and background atmospheric conditions. *J. Appl. Meteor. Climatol.*, **54**, 42–57, https://doi.org/10.1175/JAMC-D-14-0058.1.

Linn, R. R., and P. Cunningham, 2005: Numerical simulations of grass fires using a coupled atmosphere–fire model: Basic fire behavior and dependence on wind speed. *J. Geophys. Res.*, **110**, D13107, https://doi.org/10.1029/2004JD005597.

——, J. Reisner, J. J. Colman, and J. Winterkamp, 2002: Studying wildfire behavior using FIRETEC. *Int. J. Wildland Fire*, **11**, 233–246, https://doi.org/10.1071/WF02007.

Maitani, T., and E. Ohtaki, 1987: Turbulent transport processes of momentum and sensible heat in the surface layer over a paddy field. *Bound.-Layer Meteor.*, **40**, 283–293, https://doi.org/10.1007/BF00117452.

——, and R. H. Shaw, 1990: Joint probability analysis of momentum and heat fluxes at a deciduous forest. *Bound.-Layer Meteor.*, **52**, 283–300, https://doi.org/10.1007/BF00122091.

Mell, W., M. A. Jenkins, J. Gould, and P. Cheney, 2007: A physics-based approach to modelling grassland fires. *Int. J. Wildland Fire*, **16** (1), 1–22, https://doi.org/10.1071/WF06002.

——, A. Maranghides, R. McDermott, and S. Manzello, 2009: Numerical simulation and experiments of burning Douglas fir trees. *Combust. Flame*, **156**, 2023–2041, https://doi.org/10.1016/j.combustflame.2009.06.015.

Mueller, E., W. Mell, and A. Simeoni, 2014: Large eddy simulation of forest canopy flow for wildland fire modeling. *Can. J. For. Res.*, **44**, 1534–1544, https://doi.org/10.1139/cjfr-2014-0184.

Pimont, F., J.-L. Dupuy, R. R. Linn, and S. Dupont, 2009: Validation of FIRETEC wind-flows over a canopy and fuel-break. *Int. J. Wildland Fire*, **18**, 775–790, https://doi.org/10.1071/WF07130.

Poggi, D., and G. Katul, 2007: The ejection-sweep cycle over bare and forested gentle hills: A laboratory experiment. *Bound.-Layer Meteor.*, **122**, 493–515, https://doi.org/10.1007/s10546-006-9117-x.

——, A. Porporato, L. Ridolfi, J. D. Albertson, and G. G. Katul, 2004: The effect of vegetation density on canopy sub-layer turbulence. *Bound.-Layer Meteor.*, **111**, 565–587, https://doi.org/10.1023/B:BOUN.0000016576.05621.73.

Raupach, M. R., 1981: Conditional statistics of Reynolds stress in rough-wall and smooth-wall turbulent boundary layers. *J. Fluid Mech.*, **108**, 363–382, https://doi.org/10.1017/S0022112081002164.

Seto, D., C. B. Clements, and W. E. Heilman, 2013: Turbulence spectra measured during fire front passage. *Agric. For. Meteor.*, **169**, 195–210, https://doi.org/10.1016/j.agrformet.2012.09.015.

Shaw, R. H., J. Tavangar, and D. P. Ward, 1983: Structure of the Reynolds stress in a canopy layer. *J. Climate Appl. Meteor.*, **22**, 1922–1931, https://doi.org/10.1175/1520-0450(1983)022<1922:SOTRSI>2.0.CO;2.

Skowronski, N. S., K. L. Clark, M. Duveneck, and J. Hom, 2011: Three-dimensional canopy fuel loading predicted using upward and downward sensing LiDAR systems. *Remote Sens. Environ.*, **115**, 703–714, https://doi.org/10.1016/j.rse.2010.10.012.

Su, H.-B., R. H. Shaw, U. K. T. Paw, C.-H. Moeng, and P. P. Sullivan, 1998: Turbulent statistics of neutrally stratified flow within and above a sparse forest from large-eddy simulation and field observations. *Bound.-Layer Meteor.*, **88**, 363–397, https://doi.org/10.1023/A:1001108411184.

Sun, R., S. K. Krueger, M. A. Jenkins, M. A. Zulauf, and J. J. Charney, 2009: The importance of fire–atmosphere coupling and boundary-layer turbulence to wildfire spread. *Int. J. Wildland Fire*, **18**, 50–60, https://doi.org/10.1071/WF07072.

Thomas, C., and T. Foken, 2007: Flux contribution of coherent structures and its implications for the exchange of energy and matter in a tall spruce canopy. *Bound.-Layer Meteor.*, **123**, 317–337, https://doi.org/10.1007/s10546-006-9144-7.

Wallace, J. M., 2016: Quadrant analysis in turbulence research: History and evolution. *Annu. Rev. Fluid Mech.*, **48**, 131–158, https://doi.org/10.1146/annurev-fluid-122414-034550.

——, R. S. Brodkey, and H. Eckelmann, 1972: The wall region in turbulent shear flow. *J. Fluid Mech.*, **54**, 39–48, https://doi.org/10.1017/S0022112072000515.

Wilczak, J. M., S. P. Oncley, and S. A. Stage, 2001: Sonic anemometer tilt correction algorithms. *Bound.-Layer Meteor.*, **99**, 127–150, https://doi.org/10.1023/A:1018966204465.